

Citric Acid Removal from Aqueous Solution with Layered Aluminum Hydroxide Crystals

Guerra Rodríguez, Luis Eduardo

Facultad de Ciencias Aplicadas a la Industria. Universidad de Camagüey “Ignacio Agramonte Loynaz”. Circunvalación Norte, km 5.5. C.P. 74650. Camagüey, CUBA

Ventura Muñoz, Minerva

Departamento de Química, Universidad de Guadalajara, Marcelino García Barragán 1421. C.P. 44430, Guadalajara, Jalisco, MÉXICO

González Suárez, Erenio

Departamento de Ingeniería Química. Universidad Central “Martha Abreu de Las Villas”, Carretera Camajuaní km 7.5, Santa Clara, CUBA

Roselló Matas, Carmen

Departamento de Química, Facultad de Ciencias. Universidad de las Islas Baleares. Carretera Valldemossa km 7.5 Palma de Mallorca. ESPAÑA

Carbajal Arízaga, Gregorio Guadalupe*⁺

Departamento de Química, Universidad de Guadalajara, Marcelino García Barragán 1421. C.P. 44430, Guadalajara, Jalisco, MÉXICO

ABSTRACT: Aluminum hydroxide is a compound with diverse crystalline structures, some of which demonstrate the ability to remove chemicals from aqueous solutions. In this report, aluminum hydroxide with the Bayerite structure was synthesized and used to remove Citric Acid (CA). This structure was not modified under the reaction conditions where CA ranged from 2 to 6 mg of CA in 20 mL of water, the temperature ranged from 30 to 90 °C, and time ranged from 8 to 24 h. The constants in the Freundlich model indicated that adsorption is the phenomenon governing the CA capture by aluminum hydroxide. According to infrared spectroscopy data, adsorption of CA was produced by the hydrogen bond of hydroxyl groups in aluminum hydroxide with either carboxylate or carboxylic groups in CA. The highest removal of CA was 92.12% and the temperature was the only factor with an effect on the percentage of CA removal.

KEYWORDS: Citric acid; Adsorption; Separation; Aluminum hydroxide.

* To whom correspondence should be addressed.

+ E-mail: gregoriocarbajal@yahoo.com.mx

1021-9986/2018/4/153-161

9/\$/5.09

INTRODUCTION

Citric Acid (CA) is one of the most commercialized organic acids. Approximately 70% of the worldwide production of CA is used in the food industry since this acid increases the effectiveness of antimicrobial and oxidation preservatives, regulates pH, avoids color degradation, and acts as a flavor agent. In recent years, this acid has also been used to prepared advanced materials since this aids in regulating dimensions of nanoparticles [1,2].

CA is produced at the industrial level using fungal fermentation with *Aspergillus niger* of dextrose or sugar cane molasses. This fermentation is commonly conducted in submerged or surface reactors.

After fermentation, the CA produced in the liquid phase is then purified, concentrated, and crystallized. There are two established technological processes to separate and purify CA. One is the chemical precipitation using lime followed by a sulphuric acid treatment. The byproducts of this method produce inconvenient environmental impacts and increase costs since the equipment must be built with corrosion resistant materials and constant expensive maintenance are needed. The second method involves a liquid-liquid contact process using tertiary amines with low driving forces resulting in large equipment designs [3].

In addition to process and adaptation changes to produce larger amounts of CA, there is a continuous search to improve yields, energy efficiency, and environmental protection. Among these issues, the separation of CA from the complex fermentation medium is one challenge to address.

This work explored a process to remove CA from aqueous solutions with aluminum hydroxide. This proposal is based on the chemical stability of Gibbsite and Bayerite -two aluminum hydroxide minerals- against solutions of citric acid, once the citric acid solution removes isolated metals from these minerals [4,5]. On the other hand, a series of scientific reports in recent years demonstrated the ability of aluminum hydroxide powders to remove different chemical species from aqueous solutions such as iodide [6–9], heavy metals [10] and herbicides [11,12]. It has even been used as a basis to remove algae from water [8].

Another fact that led to the study of aluminum hydroxide as an alternative adsorbent of citric acid is that crystals of magnesium hydroxide have the ability to

retain carboxylic acids [13] and this ability is highly probable to be found in aluminum hydroxide once the herbicides remove this aluminum compound containing carboxylic groups [11,12]. In fact, acetate ions are strongly retained with aluminum hydroxide [6].

In this report, aluminum hydroxide nanoparticles were used as a solid matrix to remove CA from aqueous solutions. Experimental parameters to optimize the process were evaluated with the aim to propose an alternative method to remove CA.

EXPERIMENTAL SECTION

Synthesis of aluminum hydroxide

All the reagents used in these experiments were of analytical grade. The bottom-up strategy was employed to prepare the aluminum hydroxide nanoparticles. For this, a solution with 5.0485 g of $\text{Al}(\text{NO}_3)_3 \cdot 9\text{H}_2\text{O}$ and 200 mL of deionized water was prepared. Then, under magnetic stirring, a 14% ammonia solution was added dropwise until the pH reached 8.0. The resulting suspension was stirred 24 hours and then the solids were removed by decantation and washed four times with volumes of 300 mL of water. The pH in the liquid phase of the last washing was 7.0 indicating that the remaining ions were removed. The solid was dried at 70 °C, ground in a mortar, and stored in a plastic bag.

Characterization

The aluminum hydroxide powder sample and the CA adsorption products were analyzed by solid state techniques. Powder X-Ray Diffraction (XRD) measurements were conducted in a PANalytical diffractometer, model Empyrean, with a Cu source. The diffractograms were collected at a step of 0.02 degrees and 30 seconds of collection per step. InfraRed (IR) spectra were obtained in the reflectance mode using a Thermo Scientific spectrometer, model NICOLET iS5 iD5 ATR, and averaging 16 scans with resolutions of 4 cm^{-1} . The Scanning Electron Microscopy (SEM) analysis was conducted in a TESCAN microscope model MIRA 3 LMU with a field emission electron gun.

Removal of CA

The capability of removing CA from aqueous solutions was assessed with a multilevel factorial experimental design involving three factors and three

each: temperature (30, 60 and 90 °C), CA concentration (10, 20 and 30 mg/mL) and time (8, 16 and 24 h). The citric acid solutions were prepared with 200, 400, and 600 mg in 20 mL of water. The experiment was designed by triplicate and optimized from 81 runs up to 18 runs using the Optimal Design tool available on professional software Statgraphics Centurion XVI. The candidate list obtained is reported in Table 1.

The reactions were conducted in 50 mL beakers with 20 mL of water and 1.0 mg of aluminum hydroxide and the experimental conditions are described in Table 1. The vessel was then introduced in a glicerine bath and the suspension was stirred for one hour. Reactions at 90 °C were conducted in hermetically sealed in a Teflon vessel with 25 mL of volume. After the reaction, the beakers were cooled down to room temperature. The solutions were then transferred to glass flasks with screw-caps and stored in a freezer at 4 °C. After one day, the Al(OH)₃ powder was deposited on the bottom of the flask, then 1.0 mL of the liquid phase was transferred to beakers, mixed with 50 mL of water, and titrated with a NaOH solution to determine the percentage of CA removed.

Statistical analysis

Statistical analysis was conducted with Statgraphics Centurion XVI. Normality tests were done to guarantee the effectiveness of the statements. The analysis of the variance test (ANOVA) was done to determine the contribution of each reaction parameter on the percentage of CA removal in addition to the Duncan multiple range tests to determine the amount of significant difference between each mean level. The nonlinear regression tool (Marquardt estimation method) was used to fit the obtained data into the Freundlich equation model. Isothermal models were estimated for processes at 30 and 60 °C. A confidence of 95% was used in all the analysis.

RESULTS and DISCUSSION

The citric acid – aluminum hydroxide product

The solids recovered from six experiments were analyzed by XRD and FT-IR techniques. Samples were chosen to include powders from experiments subjected to the three temperature levels (30, 60 and 90 °C) combined with the two reaction times (8 and 24 h) along with the highest content of CA. The XRD results (Fig. 1) revealed a profile with low intensity reflections due to the low

content of material recovered from these experiments. In fact, the glass sample holder produced the wide pseudo-signals at 5-12 and 18-36 degrees (2theta). However, clear reflections close to 18, 20, and 40 degrees (2theta) matched the XRD profile of the Al(OH)₃ compound identified in the Bayerite structure with ICDD card number 200011. This result indicates that the aluminum hydroxide powder is stable under the experimental conditions of CA removal.

According to the literature, the Bayerite structure is a layered aluminum hydroxide similar to Gibbsite [14,15] and some related structures like that of magnesium hydroxide are capable of removing carboxylic acids through an intercalation process [13], i.e., the carboxylic acid is introduced between the layers, thus producing separation of layers easily detected by a shift of XRD reflections. The X-ray profiles in Figure 1 do not present such a shift. Therefore, the intercalation of CA did not occur. However, the removal of CA could be favored by the presence of nanopores formed by characteristic lattice voids in layers of the Bayerite structure [14].

The sample obtained from the experiment at 30 °C for 24 h contained a second crystalline phase (asterisk in Fig. 1), which was identified as aluminum oxide (ICDD card number 750278); such phase did not affect the CA removal as presented below.

The FT-IR spectrum of the pristine aluminum hydroxide (Fig. 2) contains a set of bands in the 750 and 500 cm⁻¹ regions attributed to vibrational modes involving metal-oxygen bonds in agreement with reported spectra of aluminum hydroxide [11,12]. The spectrum also presents a series of well-defined bands with low intensity between 3600 and 3400 cm⁻¹ related to the O-H stretching mode in a crystalline hydroxide structure [13]. If the aluminum hydroxide powder were amorphous, a single wide signal would appear [9,12]. A pair of bands at 1017 and 907 cm⁻¹ can be associated to the Al-O-H bending mode, which is observed in metal hydroxides [9,16,17]. Finally, a band at 1368 cm⁻¹, which could be associated to a symmetric stretching of adsorbed nitrates ions contained in the reagent to prepare the aluminum hydroxide [18,19], could also be assigned to an H-O stretching mode as observed in a gallium oxyhydroxide sample [20]; this band, although not discussed in the literature, appeared with high intensity in aluminum hydroxide samples [11,12].

Table 1: Experimental conditions to evaluate the removal of citric acid.

Block	Run	Temperature (°C)	CA concentration (mg/mL)	Time (h)
1	1	30	10	8
1	6	90	10	16
1	8	60	10	24
1	12	90	20	8
1	20	60	30	8
1	27	90	30	24
2	30	90	10	8
2	31	30	10	16
2	36	90	10	24
2	37	30	20	8
2	46	30	30	8
2	51	90	30	16
2	52	30	30	24
3	56	60	10	8
3	61	30	10	24
3	72	90	20	24
3	75	90	30	8
3	76	30	30	16
3	80	60	30	24

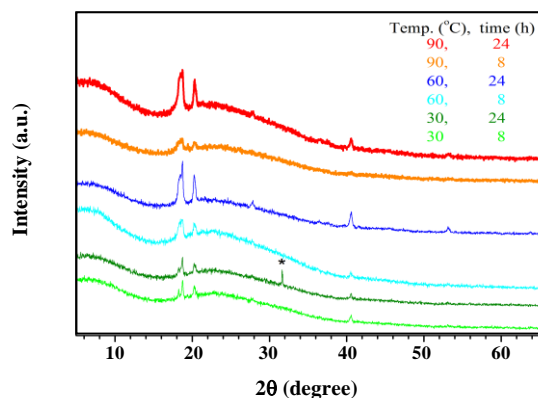


Fig. 1: X-ray diffractogram of aluminum hydroxide samples recovered after removal at 30, 60 and 90 °C after 8 and 24 hours of reaction with the highest concentration of CA.

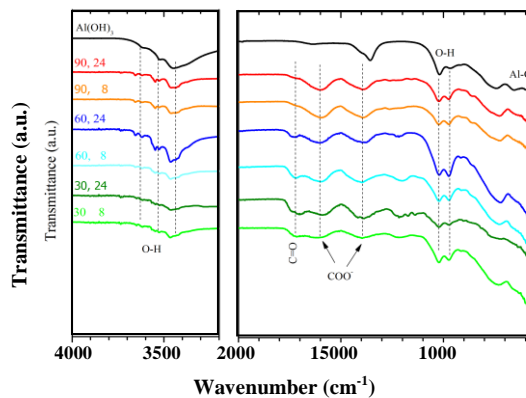


Fig. 2: Infrared spectra of aluminum hydroxide samples recovered after removal at 30, 60 and 90 °C after 8 and 24 hours of reaction with the highest concentration of CA.

The IR spectrum of pure citric acid is well-known and reported elsewhere [21,22]. This spectrum has one intense signal around 3500 cm^{-1} of O-H stretching mode and a couple of sharp intense bands at 1730 and 1700 cm^{-1}

of the stretching mode of free and H-bonding C=O groups [21].

The powder samples recovered from the CA removal experiments retain the Al-O vibration bands below 750 cm^{-1} ,

which is in agreement with XRD data indicating that the aluminum hydroxide structure is still present.

Regarding those signals produced by movements of –OH groups, the region around 3500 cm^{-1} is formed by wide overlapped bands indicating that the crystal environment of hydroxyl groups was perturbed and the reason is likely the formation of H bonds with CA. Also the intensity of the bands at 1368 and 1017 cm^{-1} decrease, thus reinforcing the statement that hydroxyl groups are involved in H bonds with CA [13]. Formation of H bonds with hydroxyl groups in fluoride adsorption experiments has also been observed [9].

The signals from CA are two intense bands at 1600 and 1400 cm^{-1} identified as the symmetric and asymmetric stretching modes of carboxylate groups, thus indicating that carboxylic groups were deprotonated [18,19]. This phenomenon occurred in the carboxylic groups in reactions at $90\text{ }^{\circ}\text{C}$ regardless of the reaction time.

On the contrary, the spectra of samples treated at 30 and $60\text{ }^{\circ}\text{C}$ presented another signal from CA at 1685 cm^{-1} , which is produced by the C=O stretching moiety in protonated carboxylic groups. It is important to note that the wavenumber of this vibration is lower than that of free carboxylic groups which appear close to 1730 cm^{-1} [21], therefore, the protonated carboxylic groups are also responsible to form H bonds with the aluminum hydroxide powder.

CA Removal

The summary statistics for response variables (percentage of CA removal) in Table 2 show success of 92.12% as a general average of removal. After considering Run “8” as an outlier, Dixon's test was performed. The small standard error in the average value is a signal of accuracy. Standard skewness and kurtosis are both below 2.0 rejecting, in principle, a non-normal behavior of variables studied. Chi-square and Shapiro-Wilk normality tests confirmed later that there were no reasons to doubt that data came from a normal distribution (Table 3).

The ANOVA test (Table 4) led the investigation to understand the factors that offer a significant contribution to response variability. In order to subsequently fit the Freundlich model, it was necessary to generate a new variable “x/m” considering the rate of the mass of adsorbate (in grams) remaining in equilibrium after each experience

Table 2: Summary statistics for “percentage of CA removal”.

Count	18
Average	92.1278
Standard deviation	3.31222
Standard error	0.780697
Minimum	86.44
Maximum	97.85
Range	11.41
Standard Skewness	-0.159996
Standard Kurtosis	-0.336541

Table 3: Tests for normality of data from “percentage of CA removal”.

Test	Statistic	P-Value
Chi-Squared	12.6667	0.178278
Shapiro-Wilk W	0.953223	0.476569

per gram of adsorbent was used in the run. The new variable “x/m” was considered in the ANOVA test once and, to the best of our knowledge, offers a more concise contribution to the “percentage of CA removal” than the mass of adsorbent and the mass of adsorbate separately. The ANOVA data (Table 4) decomposes the variability of acidity into contributions due to several factors. Since the type III sums of squares was chosen, the contribution of each factor is measured having removed the effects of all other factors.

The statistical significance of each factor was evaluated through the P-values. Since one P-value of “Temperature” was less than 0.05, this is the only factor that presents a statistically significant effect on the “% of CA Removal” with 95.0% confidence level.

A box and whiskers graph (Fig. 3) shows preliminarily that there are not relevant differences between CA removal percentages obtained above $60\text{ }^{\circ}\text{C}$, which is a remarkable result for technological purposes. This finding was validated with the Duncan multiple range test in non-homogeneous groups of CA removal at $30\text{ }^{\circ}\text{C}$ and $60\text{ }^{\circ}\text{C}$ (Inset in Fig. 3). The magnitude of the statistical difference of CA removal was 5.33% (Table 5) indicating that remarkable higher removals are not expected above $60\text{ }^{\circ}\text{C}$.

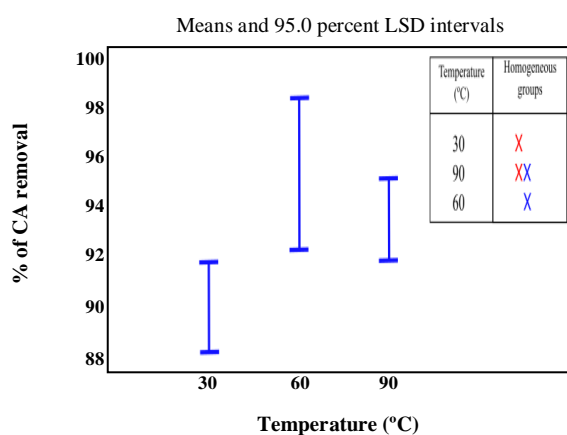
Table 4: Analysis of Variance for “% of CA Removal” - Type III Sums of Squares.

Source	Sum of Squares	Df	Mean Square	F-Ratio*	P-Value
MAIN EFFECTS					
A: x/m	5.81539	2	2.9077	0.37	0.7006
B: Temperature	73.1246	2	36.5623	4.62	0.0349
C: Time	23.8976	2	11.9488	1.51	0.2632
RESIDUAL	87.0131	11	7.91029		
TOTAL (CORRECTED)	186.503	17			

*All F-ratios are based on the residual mean square error.

Table 5: Significant difference for mean differences.

Contrast	Significant difference	Difference
30 - 60	Yes	-5.33703
30 - 90	Not	-3.53342
60 - 90	Not	1.8036

**Fig. 3: Box and whiskers graph for “% of CA Removal”.**

Modeling Freundlich's isotherms

Considering the importance of CA removal for applied purposes, it was necessary to know how accurate the results are to establish the Freundlich adsorption theory. Freundlich's model, $x/m = K c^{1/n}$ expresses the resulting equilibrium in a system where k and $1/n$ are specific constants for a particular temperature and pair adsorbent-adsorbate. Constants for two nonlinear regression models were found for 30 °C and 60 °C isotherms using the nonlinear regression tool (Marquardt estimation method) in the Statgraphics Centurion XVI software resulting:

a) For $T = 30$ °C

$x / m = 74.3368 C^{0.697138}$; R-Squared (adjusted for d.f.) = 72.3148 %, Standard error of estimation = 0.402821

b) For $T = 60$ °C

$x / m = 7.60088 C^{0.170164}$; R-Squared (adjusted for d.f.) = 76.3927 %, Standard error of estimation = 0.0330622

Estimation results and graphs are shown in Tables 6 and 7 and Figs. 4 and 5. Fitted models explain more than 70% of response variability (R-Squared) with a small standard error of estimation suggesting a good correlation with the Freundlich adsorption theory. Therefore, adsorption is the phenomenon governing CA removal by the solid aluminum hydroxide.

Since adsorption occurs through weak forces between CA and aluminum hydroxide, desorption is expected to be achieved using soft treatments. In fact, a preliminary experiment demonstrated that CA is transferred back to the liquid phase by stirring the CA-aluminum hydroxide powder in a 0.5 M Na_2CO_3 solution. However, the formal desorption study is not within the scope of the present article. These findings will be presented in a future report.

CONCLUSIONS

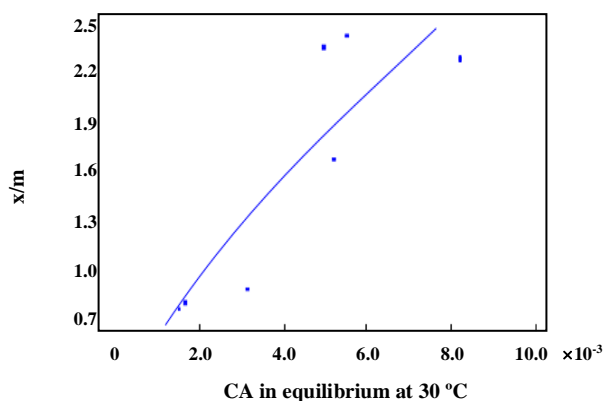
Aluminum hydroxide synthesized by precipitation with ammonium hydroxide produced a crystalline compound with the Bayerite structure. The structure was not modified under the reaction conditions where CA ranged from 10 to 30 mg/mL, the temperature ranged from 30 to 90 °C, and time ranged from 8 to 24 h.

Table 6. Estimation results for $T = 30\text{ }^{\circ}\text{C}$.

			Asymptotic	95.0%
			Confidence	Interval
Parameter	Estimate	Standard error	Lower	Upper
K	74.3368	80.9017	-133.628	282.302
1/n	0.697138	0.208009	0.162434	1.23184

Table 7: Estimation results for $T = 60\text{ }^{\circ}\text{C}$.

			Asymptotic	95.0%
			Confidence	Interval
Parameter	Estimate	Standard error	Lower	Upper
K	7.60088	3.92909	-9.30464	24.5064
1/n	0.170164	0.079662	-0.172594	0.512921

Fig. 4: X-Y plot for the fitted Freundlich model at $T = 30\text{ }^{\circ}\text{C}$.

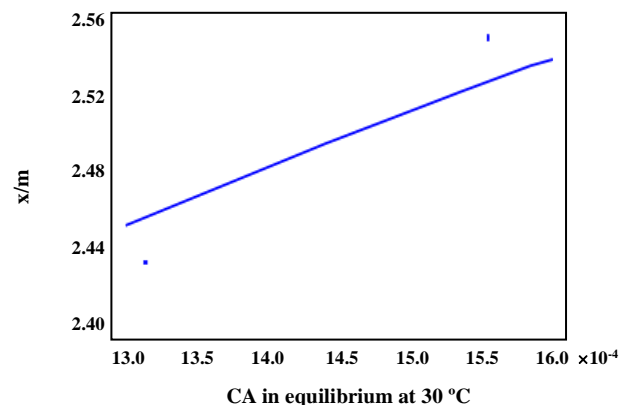
The whole deprotonation of carboxylic groups occurred at $90\text{ }^{\circ}\text{C}$ and partial deprotonation was observed at 30 and $60\text{ }^{\circ}\text{C}$. The adsorption of CA is produced by hydrogen bonds of hydroxyl groups in aluminum hydroxide with either carboxylate or carboxylic groups in CA.

The nanopores naturally occurring in the Bayerite-type sheets could favor the adsorption of CA once the well-defined sharp signal of hydroxyl groups typical of crystalline hydroxide became wider.

Aluminum hydroxide is capable of capturing 92.12% of CA contained in aqueous solutions.

The temperature is the only factor that has a statistically significant effect on the percentage of CA removal.

The statistical difference of CA removal between

Fig. 5: X-Y plot for the fitted Freundlich model at $T = 60\text{ }^{\circ}\text{C}$.

$30\text{ }^{\circ}\text{C}$ and $60\text{ }^{\circ}\text{C}$ is 5.33%, a small value that probably does not compensate for the energy cost involved. This range of temperatures must be considered in scaling the CA separation process.

Regarding the removal percentages between $60\text{ }^{\circ}\text{C}$ and $90\text{ }^{\circ}\text{C}$, no statistical difference has been observed. Therefore, it is not recommended to increase the temperature above $60\text{ }^{\circ}\text{C}$.

The Freundlich model's constants were adequately fitted for the system's equilibrium at $30\text{ }^{\circ}\text{C}$ and $60\text{ }^{\circ}\text{C}$ indicating that adsorption is the phenomenon governing the CA capture by aluminum hydroxide.

Acknowledgements

L.E.G.R. thanks the Balearic Island University for support through the project CUD 2016/09.

Received : Apr. 6, 2017 ; Accepted : Oct. 16, 2017

REFERENCES

- [1] Kamali M., Ghorashi S.A.A., Asadollahi M.A., Controllable Synthesis of Silver Nanoparticles Using Citrate as Complexing Agent: Characterization of Nanoparticles and Effect of pH on Size and Crystallinity, *Iran. J. Chem. Chem. Eng. (IJCCE)*, **31**(4): 21–28 (2012).
- [2] Alaei M., Rashidi A., Mahjoub A., Two Suitable Methods for the Preparation of Inorganic Fullerene-Like (IF) WS₂ Nanoparticles, *Iran. J. Chem. Chem. Eng. (IJCCE)*, **28**(2): 91–98 (2009).
- [3] Kudzai C.T., Ajay K., Ambika P., Citric Acid Production by *Aspergillus Niger* Using Different Substrates. *Malays. J. Microbiol.*, **12**(3): 199–204 (2016).
- [4] Boriová K., Urík M., Bujdoš M., Pífková I., Matúš P., Chemical Mimicking of Bio-Assisted Aluminium Extraction by *Aspergillus Niger*'s Exometabolites, *Environ. Pollut.*, **218**: 281–288 (2016).
- [5] Liao M., Effects of Organic Acids on Adsorption of Cadmium onto Kaolinite, Goethite, and Bayerite. *Pedosphere*, **16**(2): 185–191 (2006).
- [6] Zhang Y.-X.; Jia Y., Fluoride Adsorption onto Amorphous Aluminum Hydroxide: Roles of the Surface Acetate Anions, *J. Colloid Interface Sci.*, **483**(1): 295–306 (2016).
- [7] Ganvir V., Das K., Removal of Fluoride from Drinking Water Using Aluminum Hydroxide Coated Rice Husk Ash, *J. Hazard. Mater.*, **185**(2–3): 1287–1294 (2011).
- [8] Chen G., Peng C., Fang J., Dong Y., Zhu X., Cai H., Biosorption of Fluoride from Drinking Water Using Spent Mushroom Compost Biochar Coated with Aluminum Hydroxide, *Desalin. Water Treat.*, **57**(26): 12385–12395 (2016).
- [9] Barathi M., Kumar A.S.K., Rajesh N., Aluminium Hydroxide Impregnated Macroporous Aromatic Polymeric Resin as a Sustainable Option for Defluoridation, *J. Environ. Chem. Eng.*, **3**: 630–641 (2015).
- [10] Liu R., Ju J., He Z., Hu C., Liu H., Qu J., Utilization of Annealed Aluminum Hydroxide Waste with Incorporated Fluoride for Adsorptive Removal of Heavy Metals, *Colloids Surfaces A Physicochem. Eng. Asp.*, **504**: 95–104 (2016).
- [11] Kamaraj R., Vasudevan S., Facile One-Pot Electrosynthesis of Al(OH)₃ - Kinetics and Equilibrium Modeling for Adsorption of 2,4,5-Trichlorophenoxyacetic Acid from Aqueous Solution, *New J. Chem.*, **40**: 2249–2258 (2016).
- [12] Kamaraj R., Davidson D.J., Sozhan G., Vasudevan S., Adsorption of Herbicide 2-(2,4-Dichlorophenoxy) Propanoic Acid by Electrochemically Generated Aluminum Hydroxides: An Alternative to Chemical Dosing, *RSC Adv.*, **5**: 39799–39809 (2015).
- [13] Wypych F., Arízaga G.G.C., Intercalation and Functionalization of Brucite with Carboxylic Acids | Intercalação E Funcionalização Da Brucita Com Ácidos Carboxílicos, *Quim. Nova*, **28**(1): 24–29 (2005).
- [14] Demichelis R., Civalleri B., Noel Y., Meyer A., Dovesi R., Structure and Stability of Aluminium Trihydroxides Bayerite and Gibbsite: A Quantum Mechanical Ab Initio Study with the Crystal06 Code. *Chem. Phys. Lett.*, **465**(4–6): 220–225 (2008).
- [15] Vitaly P. Isupov, Lyudmila E. Chupakhina, Raisa P. Mitrofanova, K. A. T., Synthesis, Structure, Properties, and Application of Aluminium Hydroxide Intercalation Compounds, *Chem. Sustain. Dev.*, **8**: 121–127 (2000).
- [16] Liu X., Qiu G., Zhao Y., Zhang N., Yi R., Gallium Oxide Nanorods by the Conversion of Gallium Oxide Hydroxide Nanorods, *J. Alloys Compd.*, **439**(1–2): 275–278 (2007).
- [17] Lee I., Kwak J., Haam S., Lee S.Y., Dipeptide-Assisted Growth of Uniform Gallium Oxohydroxide Spindles, *J. Cryst. Growth*, **312**(14): 2107–2112 (2010).
- [18] Wypych F., Arízaga G.G.C., da Costa Gardolinski J.E.F., Intercalation and Functionalization of Zinc Hydroxide Nitrate with Mono- and Dicarboxylic Acids, *J. Colloid Interface Sci.*, **283**(1): 130–138 (2005).
- [19] Arizaga G.G.C., Mangrich A.S., da Costa Gardolinski J.E.F., Wypych F., Chemical Modification of Zinc Hydroxide Nitrate and Zn-Al-Layered Double Hydroxide with Dicarboxylic Acids, *J. Colloid Interface Sci.*, **320**(1): 168–176 (2008).
- [20] Reddy L.S., Ko Y.H., Yu J.S., Hydrothermal Synthesis and Photocatalytic Property of β -Ga₂O₃ Nanorods, *Nanoscale Res. Lett.*, **10**(1): 364 (2015).

- [21] Azeredo H.M.C., Kontou-Vrettou C., Moates G.K., Wellner N., Cross K., Pereira P.H.F., Waldron K.W., **Wheat Straw Hemicellulose Films as Affected by Citric Acid**, *Food Hydrocoll.*, **50**:1–6 (2015).
- [22] Zhao J.P., Liu X.R., Qiang L.S., **Characteristics of the Precursors and Their Thermal Decomposition during the Preparation of LiNbO₃ Thin Films by the Pechini Method**, *Thin Solid Films*, **515**(4): 1455–1460 (2006).